ACADEMIC
PRESS

Down-regulation of transcription of the proapoptotic gene BNip3 in cultured astrocytes by murine coronavirus infection

Yingyun Cai, Yin Liu, Dongdong Yu, and Xuming Zhang*

Department of Microbiology and Immunology, University of Arkansas for Medical Sciences, 4301 W. Markham Street, Slot 511, Little Rock, AR 72205

Abstract

Murine coronavirus mouse hepatitis virus (MHV) causes encephalitis and demyelination in the central nervous system of susceptible rodents. Astrocytes are the major target for MHV persistence. However, the mechanisms by which astrocytes survive MHV infection and permit viral persistence are not known. Here we performed DNA microarray analysis on differential gene expression in astrocyte DBT cells by MHV infection and found that the mRNA of the proapoptotic gene BNip3 was significantly decreased following MHV infection. This finding was further confirmed by quantitative reverse transcription–polymerase chain reaction, Western blot analysis, and BNip3-promoter-luciferase reporter system. Interestingly, infection with live and ultraviolet light-inactivated viruses equally repressed BNip3 expression, indicating that the down-regulation of BNip3 expression does not require virus replication and is mediated during cell entry. Furthermore, treatment of cells with chloroquine, which blocks the acidification of endosomes, significantly inhibited the repression of the BNip3 promoter activity induced by the acidic pH-dependent MHV mutant OBLV60, which enters cells via endocytosis, indicating that the down-regulation of BNip3 expression is mediated by fusion between viral envelope and cell membranes during entry. Deletion analysis showed that the sequence between nucleotides 262 and 550 of the 588-base-pair BNip3 promoter is necessary and sufficient for driving the BNip3 expression and that it contains signals that are responsible for MHV-induced down-regulation of BNip3 expression in DBT cells. These results may provide insights into the mechanisms by which MHV evades host antiviral defense and promotes cell survival, thereby allowing its persistence in the host astrocytes.
© 2003 Elsevier Inc. All rights reserved.

Introduction

Viruses can cause different types or patterns of infection in susceptible hosts; host cells in turn respond to viral infection in many different ways. Some virus-infected cells undergo rapid destruction, whereas others become immortalized. In addition to immune response, host cells often devise countermeasure mechanisms against virus invasion. One of the common antiviral defense strategies operated by host cells is programmed cell death or apoptosis, for apoptosis would eliminate virus-infected cells, thereby blocking the production of progeny virus and limiting the spread of virus to neighboring uninfected cells. However, apoptosis can also be a viral strategy to invade hosts. Many viruses can induce apoptosis in host cells during late stages of the

virus life cycle to speed up their release from infected cells and spread to neighboring cells. On the other hand, many viruses have also devised strategies to counter host antiviral defense by inducing an antiapoptotic state in host cells. For examples, human immunodeficiency virus tat protein (Zauli et al., 1995) and Epstein–Barr virus-EBNA4 and -LMP-1 proteins (Silins and Sculley, 1995; Henderson et al., 1991) induce the expression of antiapoptotic protein Bcl-2, which is the master checkpoint protein of apoptosis through the mitochondrial pathway (Hockenbery et al., 1990). Members of the Bcl-2 family share up to four conserved regions of homology known as Bcl-2 homology (BH) domains, which mediate interactions among themselves (Kelekar and Thompson, 1998). A delicate balance of interaction between proapoptotic and antiapoptotic members of the Bcl-2 family has been shown to modulate the sensitivity of cells to mitochondrial integrity in response to apoptotic signals (Shimizu et al., 1999). Many viral proteins are Bcl-2 ho-

* Corresponding author. Fax: +1-501-686-5359.
E-mail address: zhangxuming@uams.edu (X. Zhang).

mologs such as adenovirus E1B 19-kDa protein (Ad-E1B 19K) (Chiou et al., 1994).

BNip3 (Bcl-2 and Nineteen-kilodakton-protein interacting protein 3) is the proapoptotic member of the Bcl-2 family. It was first identified as an Ad-E1B 19K and Bcl-2 interacting protein (Boyd et al., 1994). BNip3 contains only the BH3 domain (Yasuda et al., 1998). It functions as a proapoptotic protein that both induces apoptosis and increases the sensitivity of cells to apoptosis induced by drugs and granzymes B upon transient expression (Chen et al., 1997). Moreover, BNip3 can form heterodimers with anti-apoptotic Bcl-2 family members such as Bcl-2 and Bcl-$_{XL}$ and promotes apoptosis by sequestering the antiapoptotic members (Imazu et al., 1999). Recent evidence from studies in T cells suggests that the BH3-dependent apoptotic pathways can also be turned on by surface receptor via interaction with CD47 (Lamy et al., 2003). It has been reported that the expression of BNip3 gene is induced by hypoxia (Bruick, 2000; Kubasiak et al., 2002) and a zinc-finger protein, PLAGL2 (Mizutani et al., 2002), leading to cellular apoptosis.

Murine coronavirus mouse hepatitis virus (MHV) is an enveloped, positive-strand RNA virus. It contains four or five structural proteins, depending on virus strains. The spike protein (S) is the major peplomer protruding from the virion envelope. It is responsible for virion attachment to host cells via interaction with receptors, induction of fusion between viral envelope and cell membranes during infection, and elicitation of neutralizing antibodies and cellular immune responses (Lai, 1990). Thus, the S protein is essential for virus infectivity. The hemagglutinin/esterase (HE) has sequence homology with the HEF protein of influenza C virus (Luytjes et al., 1988). It contains an esterase activity but lacks the receptor-binding activity (Yokomori et al., 1989). It is present on the virion surface only in some MHV strains (such as JHM) but not others (such as A59) (Shieh et al., 1989; La Monica et al., 1992), and it is thus not essential for virus infectivity. The small envelope (E) protein is acetylated (Yu et al., 1994) and the membrane (M) protein is glycosylated (Niemann et al., 1984). Both proteins are hydrophobic and largely embedded in the virion envelope. They are essential for virion assembly and morphogenesis (Vennema et al., 1996; Bos et al., 1996). The nucleocapsid (N) protein is a phosphoprotein that is tightly associated with the viral RNA genome to form the nucleocapsid inside the envelope shell (Stohlman and Lai, 1979). It has been shown that dephosphorylation of the N protein following viral entry into host cells is a prerequisite step for virus replication (Kalicharran and Dales, 1995; Kalicharran et al., 1996).

During the initiation of virus infection, the S protein binds to a specific receptor on the surface of susceptible cells, which is a murine biliary glycoprotein belonging to the carcinoembryonic antigen (CEA) in the immunoglobulin superfamily (Williams et al., 1991). Upon viral binding, fusion between viral envelope and plasma membrane is then triggered, allowing the nucleocapsid to release into the cytoplasm. Interaction between the S protein and the receptor can also mediate endocytosis (Nash and Buchmeier, 1997). In this case, fusion occurs between viral envelope and endosomal membrane at an acidic environment. Once in the cytoplasm, the N protein is presumably dephosphorylated and dissociates from the genomic RNA, thereby completing the uncoating process. The viral RNA-dependent RNA polymerase is then translated from the incoming viral genome and viral replication proceeds subsequently.

MHV infects rodents, causing hepatitis, nephritis, enteritis, and central nervous system (CNS) diseases. Infection of rodent CNS results in encephalitis and demyelination, the latter of which resembles the multiple sclerosis seen in humans (Lampert et al., 1973; Herndon et al., 1977). Therefore, MHV has been extensively used as an animal model for studying the pathogenesis of multiple sclerosis and other CNS degenerative diseases. In certain mouse strains, demyelination develops during the first week of infection (Woyciechowska et al., 1984) and reaches to a peak at approximately 30 days postinfection (p.i.), at which time infectious virus can no longer be isolated but viral RNAs are still detectable (Fleming et al., 1993; Adami et al., 1995). The predominant cell type in the CNS for harboring persistent viruses is the astrocyte (Perlman and Ries, 1987). Indeed, persistent infection can be readily established in animal CNS (Adami et al., 1995; Rowe et al., 1998) and cultured astrocytes (Maeda et al., 1995; Chen and Baric, 1995). In contrast to the infection in vivo, infectious virus can be recovered from infected, cultured astrocytes after continuous passage of cells for more than 100 days (Chen and Baric, 1995). Because astrocyte is one of the antigen-presenting cells in the CNS (Fierz et al., 1985), it can produce diverse proinflammatory molecules such as cytokines, chemokines, and nitric oxide upon stimulation (Van Wagoner and Benveniste, 1999; Huang et al., 2000; Chen and Swanson, 2003). It has been shown that coronaviruses induce the expression of transforming necrosis factor- (TNF) α, interleukin- (IL) 6, matrix metalloproteinases, and inducible nitric oxide synthase in primary and established astrocytes (Joseph et al., 1993; Zhou et al., 2001; Grzybicki et al., 1997; Kyuwa et al., 1994). Thus, it is conceivable that infection of astrocytes with MHV can modulate the development of the CNS pathology and alter the course of the disease. In the past, most studies have been focused on how MHV has evolved during persistent infection in the CNS and in cultured cells (Adami et al., 1995; Rowe et al., 1998). Information on coevolvement of the host has been limited to the alteration of receptors by MHV infection (Chen and Baric, 1996; Sawicki et al., 1995).

To understand how MHV infection alters the gene expression of astrocytes, we employed the DNA microarray technology to analyze the mRNA expression profiles in MHV-infected murine astrocytoma cell line DBT and compared them with those in mock-infected DBT cells. We found that the expression of a substantial number of genes

was either increased or decreased upon MHV infection. Of these, the expression of the proapoptotic gene BNip3 was significantly decreased. A series of subsequent experiments further confirmed this conclusion. Interestingly, the down-regulation of BNip3 expression does not require viral replication and is mediated during cell entry. Our results may provide insight into the mechanisms by which MHV evades host antiviral defense and promotes cell survival, thereby allowing its persistence in the host astrocyte.

Results

MHV infection induced down-regulation of proapoptotic BNip3 gene expression in cultured astrocytes

To determine altered gene expression of DBT cells by virus infection, DBT cells were infected with MHV strain JHM at an m.o.i. of 2 or mock-infected. At 12 h p.i., intracellular RNAs were isolated with the RNAeasy kit (Qiagen Inc.). The mRNA expression profiles were determined using the Affymetrix GeneChip—the Murine Genome U74Av2 Array, which contains oligonucleotides representing approximately 8000 known genes and 4000 EST of the mouse genome. A ≥2-fold difference in mRNA amount between virus-infected and mock-infected cells was considered statistically significant. Based on this criteria, we identified 125 known genes that were significantly up-regulated by MHV infection and 124 known genes that were significantly down-regulated (data not shown). Among those, we found that the mRNA of the proapoptotic gene BNip3 was decreased approximately 2.4-fold in MHV-infected DBT cells as compared to that in mock-infected DBT cell.

To verify this microarray data, we employed three different approaches. The first approach was to use reverse transcription–polymerase chain reaction (RT–PCR) to directly measure the amounts of the BNip3 mRNA expression during the course of virus infection. DBT cells were infected with MHV strain JHM at an m.o.i. of 5. At 4, 8, and 12 h p.i., intracellular RNAs were isolated and cDNAs were synthesized by RT with a hexomer random primer. cDNAs were then amplified by PCR using a primer pair specific to BNip3 (Fig. 1A). We found that cDNAs representing the BNip3 gene decreased at 8 and 12 h p.i. in virus-infected cells as compared to those in mock-infected cells after normalizing with β-actin gene (data not shown).

To further provide quantitative assessment on the extent of BNip3 mRNA reduction by MHV infection, we employed a competitive RT–PCR. As depicted in Fig. 1A, we generated a competitor DNA fragment that contains an internal deletion of about 100 nt but which contains the same two primer binding sites on the target DNA. As the result, the amount of the target DNA fragment being amplified by PCR would be decreased with an increased amount of competitor DNA being added in the PCR reac-
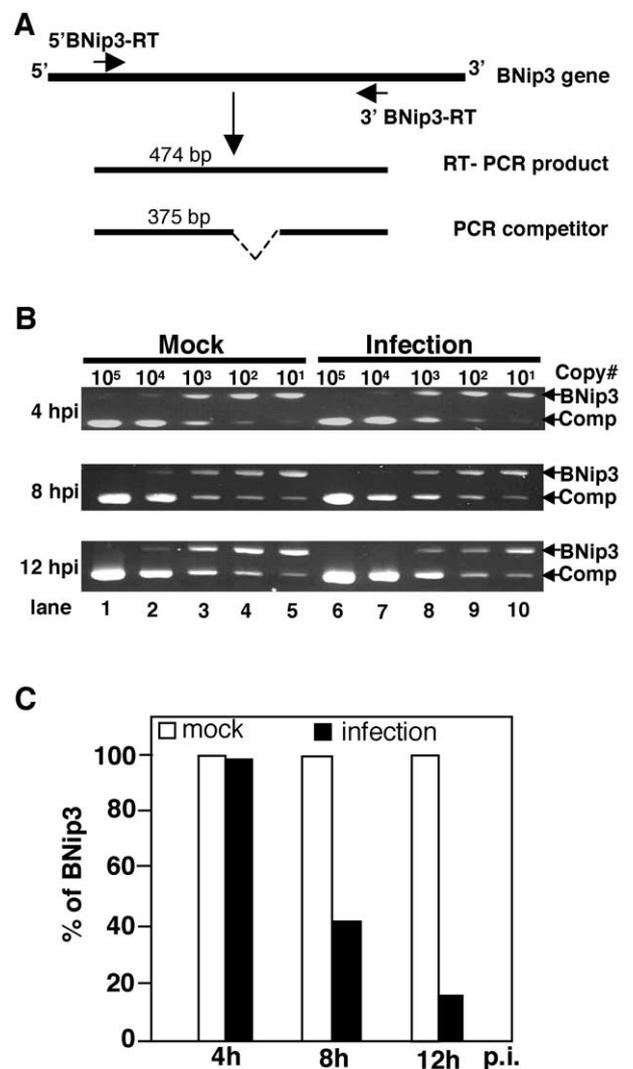

Fig. 1. Suppression of BNip3 mRNA transcription by MHV infection. (A) Schematic diagram showing the positions and directions of the primers relative to the BNip3 mRNA template used in RT–PCR. The structure and size of the target RT–PCR product and of the competitor are also shown. (B) Competitive RT–PCR results. DBT cells were infected with MHV-JHM at an m.o.i. of 5 or mock-infected. At 4, 8, and 12 h p.i., intracellular RNAs were isolated and were subjected to RT with a random primer. cDNAs were amplified by PCR using the primer pair specific to BNip3 as shown in A in the presence of a known amount of the competitor DNA. The competitor DNA was amplified from a deletion construct and was purified from agarose gel. From lanes 1 to 5 and 6 to 10, a 10-fold serially diluted competitor DNA (indicated as copy number) was added to the PCR. The RT–PCR products were analyzed by electrophoresis in 2% agarose gel and visualized by staining with ethidium bromide. Images were taken with the digital camera (UVP). The intensity of each band was determined with the software (Labworks4). Arrows indicate the target PCR products (BNip3) and the competitor PCR product (Comp), respectively. An equal amount of the target PCR product to the competitor PCR product is considered the amount of the target template in the original RNA sample, which is expressed as percentage of virus-infected samples to mock-infected samples as shown in C.

tion. The PCR products were analyzed by agarose gel electrophoresis and the intensity of the DNA bands following ethidium bromide staining was determined by densitometry.
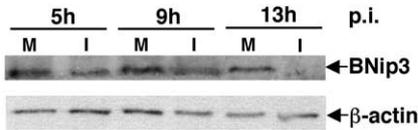
Fig. 2. Reduction of BNip3 protein expression by MHV infection. DBT cells were infected with MHV-JHM at an m.o.i. of 5 or mock-infected. At 5, 9, and 13 h p.i., the cells were harvested and lysed. Equal amounts of cell lysates were immunoprecipitated with an antibody specific to BNip3 and protein G-Sepharose beads. The precipitates were separated by polyacrylamide gel (12%) electrophoresis. Proteins were then transfered to nitrocellulose membranes and were detected with the same BNip3 antibody and enhanced chemiluminescence by Western blot analysis. An aliquot of an equal amount of cell lysates for each sample was used for analyzing the β-actin protein with the β-actin-specific antibody in Western blot as an internal control. The data are representative of three experiments. M, lysates from mock-infected cells; I, lysates from virus-infected cells.

A representative gel is shown in Fig. 1B. The amounts of the target DNAs and competitor DNAs were then plotted, and the value, at which an equal amount of target and competitor DNAs was obtained, was considered to be the amount of the target gene. To insure that the PCR products quantitatively reflected on the target gene, we optimized the PCR reaction by reducing the amount of input cDNA and the number of PCR cycles so that the amount of the DNA in each band was not saturated by ethidium bromide staining. We used this technique to determine the amount of BNip3 mRNAs at different time points p.i. As shown in Fig. 1C, there was virtually no difference in the amount of BNip3 cDNA between virus-infected and mock-infected cells at 4 h p.i., but an approximately 60% reduction was detected in virus-infected cells at 8 h p.i., as compared with that of mock-infected cells. At 12 h p.i., the reduction in BNip3 gene reached to approximately 80% in virus-infected cells. These results were reproducible in at least three independent experiments. These results demonstrate that MHV infection down-regulated BNip3 gene expression at the transcriptional level, thus confirming the results from the DNA microarray analysis.

The second approach was to determine the expression of the BNip3 protein. We employed Western blot in combination with immunoprecipitation to determine the BNip3 protein expression at various time points p.i. As expected, a slight decrease in BNip3 protein was detected in virus-infected cells at 5 and 9 h p.i., as compared to those in mock-infected cells (Fig. 2). The reduction of BNip3 protein in virus-infected cells was more pronounced at 13 h p.i., when normalized with the β-actin protein. Although the degree of reduction of the BNip3 protein in MHV-infected cells varied among experiments, the pattern of reduction was consistent in several independent experiments. These results indicate that, consistent with the pattern of mRNA expression, BNip3 protein expression was inhibited by MHV infection.

The third approach was to use a reporter system to determine the promoter activity of the BNip3 gene in re-

sponse to MHV infection. The 5′ upstream sequence (promoter) of the BNip3 gene was placed in front of the firefly luciferase gene in the pGL-BNip3 construct (Fig. 3A) (Bruick, 2000). Transient transfection of the pGL-BNip3 DNA into DBT cells that were either infected with MHV at
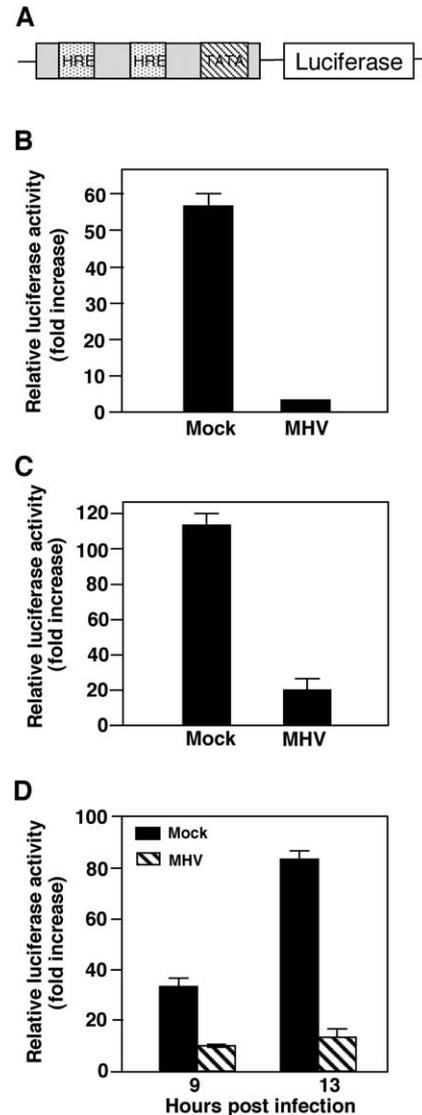

Fig. 3. Down-regulation of BNip3 promoter activity by MHV infection. (A) Schematic diagram of the BNip3 promoter-luciferase reporter plasmid pGL3-BNip3. Only the promoter and the reporter gene are shown. HRE, hypoxia response element; TATA, TATA box. (B) Luciferase activities. DBT cells were infected with MHV JHM at an m.o.i. of 5 or mock-infected. At 1 h postinfection (p.i.), cells were transfected with 500 ng of pGL3-BNip3 plasmid or the promoterless plasmid pGL3. At 18 h p.i., cell lysates were harvested and luciferase activities measured as described under Materials and methods. The relative luciferase activity in pGL3-BNip3-transfected cells is expressed as fold increase over the luciferase activity in cells transfected with the promoteless pGL3. Data indicate the means of three separate infection/transfection results. Error bars denote standard deviations. The data are representative of six independent experiments. (C) Same as in B, except that the virus was purified through sucrose-gradient ultracentrifugation. (D) Same as in B, except that the transfection was carried out 5 h prior to virus infection and the luciferase activity was determined at 9 and 13 h p.i.

an m.o.i. of 5 or mock-infected as a control resulted in the expression of luciferase activity. Consistent with the results from DNA microarray, RT–PCR and protein detection described above, the luciferase activity was significantly decreased following MHV infection (Fig. 3B). This result was reproducible in more than 20 independent transfection–infection experiments. It was also confirmed by using purified virus and UV-irradiated virus (see below). These data thus unequivocally establish that MHV infection down-regulated BNip3 gene expression in DBT cells. Because the luciferase reporter system is a very sensitive assay that has been well established and widely used for determining promoter activity and because our results also demonstrated its sensitivity and utility, we used this reporter system as a standard method for all subsequent experiments.

Because our original DNA microarray study used RNA samples isolated from DBT cells that were cultured or infected with MHV in the presence of 0.5% newborn calf serum, it is possible that the presence of a low level of serum and other unidentified factors secreted by infected-DBT cells in the inoculum might have contributed to the observed down-regulation of BNip3 expression. To rule out this possibility, we used the virus purified through sucrose gradient ultracentrifugation. As shown in Fig. 3C, infection of DBT cells with purified virus resulted in a six-fold decrease of luciferase activity as compared to that from mock-infected cells. This result is comparable to that obtained with unpurified virus (Fig. 3B), indicating that the down-regulation of BNip3 gene expression specifically resulted from MHV infection and not from factors present in the viral inoculum.

It is also possible that the observed reduction in luciferase activity resulted from inhibition of transfection efficiency by virus infection rather than from direct virus infection because MHV infection could potentially cause alteration of cell membrane permeability. To exclude this possibility, we carried out DNA transfection for 5 h to allow complete delivery of the plasmid DNA into cells prior to virus infection. We found that a significant reduction of luciferase activity was detected in MHV-infected cells as compared to mock-infected cells (Fig. 3D), although the fold reduction in luciferase activity was less prominent when compared with the results from prior infection (Fig. 3C). These data argue against an indirect effect by DNA transfection efficiency.

The down-regulation of BNip3 gene expression is specifically mediated by MHV and does not require virus replication

It is known that productive MHV replication results in inhibition of host cell translation (Tahara et al., 1994; Hilton et al., 1986). To establish that the reduction of luciferase activity expressed from the pGL3-Luc reporter was not due to MHV-replication-induced inhibition of cell translation, DBT cells were infected with UV-irradiated MHV at an
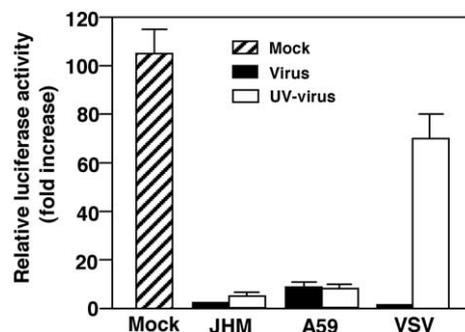

Fig. 4. Down-regulation of BNip3 promoter activity is specifically mediated by MHV infection and requires no virus replication. DBT cells were infected with MHV JHM, A59, VSV, or the respective UV-irradiated viruses. Mock-infected cells were used as controls. At 1 h p.i., cells were transfected with 500 ng of pGL3-BNip3 plasmid or of the promoterless pGL3. At 18 h p.i., cell lysates were harvested and luciferase activities measured as described under Materials and methods. The relative luciferase activity in pGL3-BNip3-transfected cells is expressed as fold increase over the luciferase activity in cells transfected with the promoteless pGL3. Date indicate the means of three separate infection/transfection results. Error bars denote standand deviations.

m.o.i. of 5 for 1 h and then transfected with the pGL3-Luc reporter DNA. Mock-infected cells were used as controls. As shown in Fig. 4, luciferase activities were reduced at similar levels in cells infected with live virus and UV-inactivated virus as compared to those in mock-infected cells. This result strongly supports the conclusion that the bulk of the reduction of luciferase activity in MHV-infected cells indeed resulted from MHV infection and not from indirect, general inhibition of cellular translation.

To establish further the specificity of the down-regulation of BNip3 gene expression, we used vesicular stomatitis virus (VSV) in a parallel experiment, because VSV is also an enveloped RNA virus whose infection has a broad host cell range and is mediated by the interaction between the envelope G protein and cell membranes (Riedel et al., 1984). As expected, the luciferase activity was completely inhibited by infection with live VSV because it is known that VSV replication shuts down host cell transcription (Fig. 4). In contrast, little reduction of luciferase activity was detected in DBT cells that were infected with UV-inactivated VSV. Nevertheless, the difference in reduction of luciferase activity between UV-inactivated MHV and VSV was significant (Fig. 4). Taken together, these results demonstrate that the down-regulation of BNip3 gene expression resulted specifically from MHV infection.

Because UV-irradiated viruses are no longer capable of replicating themselves, although they are still able to bind cell receptors and to be up-taken by the cells, UV-irradiation of viruses can be used to distinguish the involvement of various steps either before or after virus replication. The data presented in Fig. 4 also indicate that the down-regulation of BNip3 gene expression does not require virus replication. This result was reproducible in both neurotropic MHV strains JHM and A59 and in at least six independent

experiments with triplicates for each experiment (representative data shown in Fig. 4, further data not shown). These results thus establish that MHV infection induces the down-regulation of BNip3 gene expression during early stages of the virus life cycle and requires no virus replication.

Virus-cell fusion during entry induced the down-regulation of the BNip3 gene expression

As the above results pinpointed the involvement of virus entry in regulation of BNip3 gene expression, we were interested in further dissecting the individual steps of the infectious process. We designed experiments to first block downstream processes so that the role of upstream events can be assessed. However, most MHV strains, including JHM and A59, enter cells both via fusion with plasma and endosomal membranes (Nash and Buchmeier, 1997). This property poses a technical dilemma for not being able to block fusion by the common lysosomotropic agents. Gallagher et al. (1991) isolated several mutants from OBL20 cells persistently infected with MHV JHM (MHV-4). One of these mutant isolates, OBLV60, strictly depends on acidic pH for entry and infectivity. We therefore used this pH-dependent mutant for this purpose. DBT cells were transfected with the pBNip3-Luc reporter plasmid DNA for 5 h, treated with 0, 25, and 50 μM of chloroquine for 1 h prior to virus infection, and then infected with OBLV60 or the wild-type JHM at an m.o.i. of 5 in the presence of chloroquine. At 13 h p.i., cell lysates were isolated and luciferase activity determined. Mock-infected and untreated cells were used as controls. As shown in Fig. 5, treatment of cells with an increasing concentration of chloroquine resulted in an increase of luciferase activities by approximately three fold in OBLV60 infected cells (Fig. 5A), concomitant with a decrease of virus titer (Fig. 5B). In contrast, neither the luciferase activities nor the virus titers were significantly affected by chloroquine treatment in JHM-infected DBT cells. These results suggest that fusion between viral envelope and endosomal membranes during OBLV60 infection provides at least in part the signal(s) that triggers the down-regulation of BNip3 gene expression. By extrapolating the data from the mutant virus, we can envision that fusion between viral envelope and plasma/endosomal membranes during wild-type MHV infection is involved in the down-regulation of BNip3 gene expression.

Mapping the cis-acting, MHV-responsive elements in the promoter region of BNip3 gene

The above results suggest that the promoter region of the BNip3 gene contains both the cis-acting elements that are essential for BNip3 expression and the negative elements that repress BNip3 expression in response to MHV infection. To identify and dissect such cis-acting elements, we made a series of reporter constructs that contain various deletions in the BNip3 promoter. In an initial experiment,
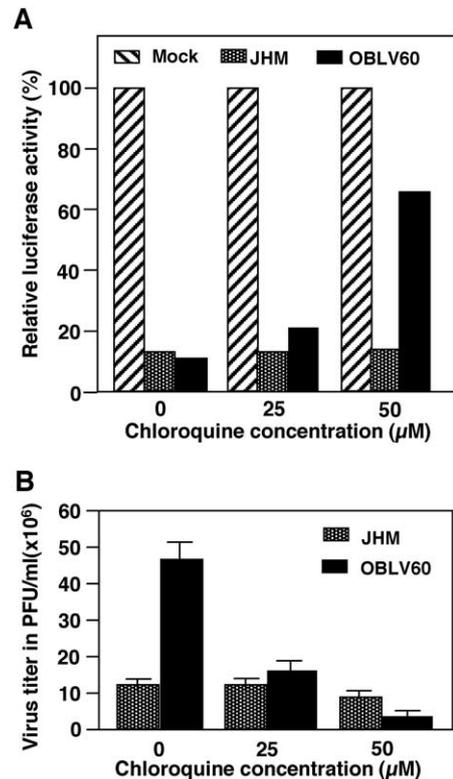

Fig. 5. Chloroquine treatment blocked the down-regulation of BNip3 promoter activity mediated by infection with the mutant OBLV60 in a dose-dependent manner. DBT cells were transfected with pGL3-BNip3 for 6 h and then infected with purified wild-type JHM or mutant OBLV60 at an m.o.i. of 5. Chloroquine was added to the DBT cells 1 h prior to infection and was present throughout the infection. At 13 h p.i. (19 h posttransfection), cell lysates were harvested. One set of the lysates was subjected to luciferase assay for determining the luciferase activity (A) and the other set to virus plaque assay for determining virus titers (B). The relative luciferase activity in JHM- and OBLV60-infected cells is expressed as percentage of the luciferase activity in mock-infected cells. Data indicate the means of three separate infection/transfection results. Error bars denote standard deviations.

we determined the minimal promoter sequences required for BNip3 gene expression. DBT cells were transfected with various deletion reporter constructs. Transfection with the promoterless vector was used as a negative (basal level) control. At 18 h posttransfection, cells were lysed and assayed for luciferase activities. As summarized in Fig. 6, when deletions were made from the 5′-end to nt 262 (construct Pr-7) and from nt 91 to 262 (construct Pr-6) of the promoter, the luciferase activities retained at 91.5 and 71.1%, respectively, as compared to the full-length promoter, indicating that the upstream half (262 nt) of the promoter is not essential for BNip3 gene expression. In contrast, deletions of nt 262 to 550 (in constructs Pr-4 and Pr-5) essentially abolished the luciferase activity, indicating that the sequence from nt 262 to 550 of the promoter is the cis-acting element required for driving BNip3 gene expression. Further deletion of the downstream sequence (from nt 550 to 591 in Pr-10) resulted in approximately 50% reduc-

A

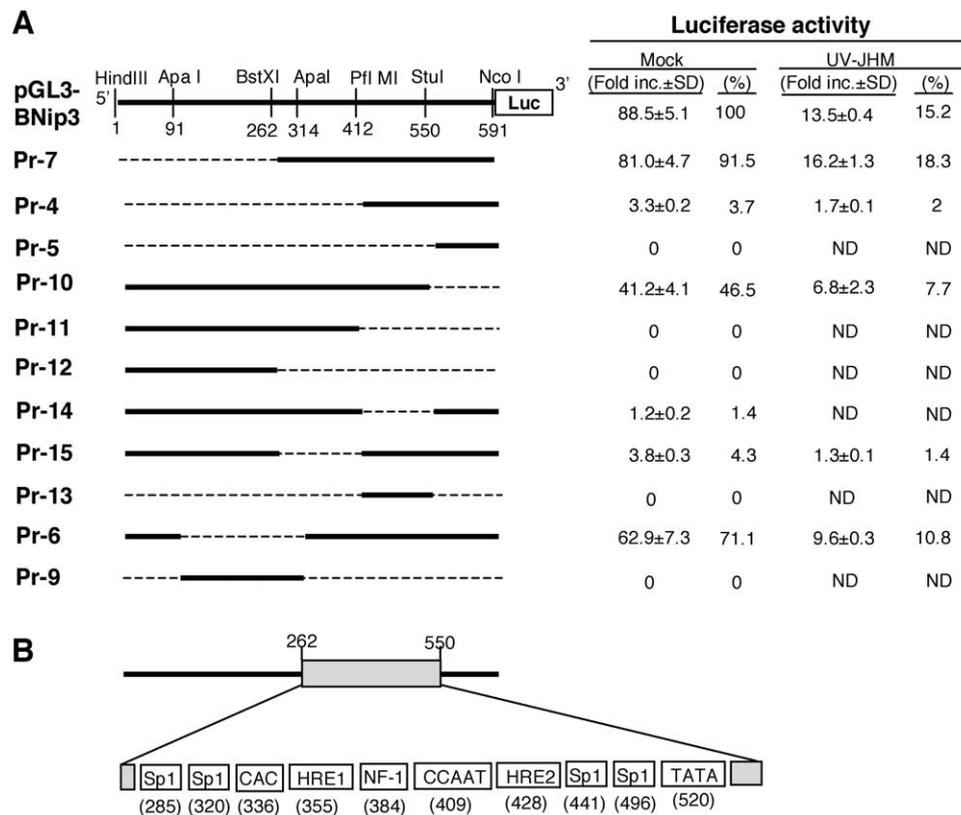|	Luciferase activity				
	Mock		UV-JHM		
	(Fold inc.±SD)	(%)	(Fold inc.±SD)	(%)	
pGL3-BNip3	88.5±5.1	100	13.5±0.4	15.2	
Pr-7	81.0±4.7	91.5	16.2±1.3	18.3	
Pr-4	3.3±0.2	3.7	1.7±0.1	2	
Pr-5	0	0	ND	ND	
Pr-10	41.2±4.1	46.5	6.8±2.3	7.7	
Pr-11	0	0	ND	ND	
Pr-12	0	0	ND	ND	
Pr-14	1.2±0.2	1.4	ND	ND	
Pr-15	3.8±0.3	4.3	1.3±0.1	1.4	
Pr-13	0	0	ND	ND	
Pr-6	62.9±7.3	71.1	9.6±0.3	10.8	
Pr-9	0	0	ND	ND	

B

Fig. 6. Mapping the cis-acting elements of the BNip3 promoter. (A) Summary of the deletion mapping results. On the left is the schematic diagram showing the structure of the BNip3 promoter in various luciferase (Luc) reporter constructs (indicated on the far left). The restriction enzymes used for construction of the plasmids and the positions (nt) of their recognition sites are indicated at the top. Bold lines denote the presence of the sequences, whereas dashed lines denote the deleted sequences. On the right shows the results of the luciferase activities. DBT cells were transfected with various reporter constructs for 5 h and then infected with UV-inactivated MHV strain JHM (UV-JHM) or mock-infected (Mock). At 18 h posttransfection, cells were lysed and assayed for luciferase activity. The luciferase activity was expressed as fold increase over that expressed from the promoterless pGL3. The data were the means and standard deviations (SD) of at least three independent experiments. The luciferase activities for the deletion constructs were also expressed as percentage to that derived from mock-infected and full-length plasmid-transfected cells, which was set as 100%. (B) Details of the cis-acting elements in the BNip3 promoter region between nt 262 and 550. The sequence was analysed with the computer software Signal Scan (Prestridge, 2000). The putative consensus sequences for the binding of transcription factors are shown schematically. The numbers in brackets indicate the approximate nt positions in the promoter.

tion of luciferase activity, suggesting that this sequence can influence the transcription efficiency but is not essential for BNip3 gene expression. Partial or complete deletions of the 288-nt sequence (from nt 262 to 550) in constructs Pr-11, Pr-12, Pr-14, Pr-15, Pr-13, and Pr-9 essentially abolished the luciferase activity. We thus conclude that the 288-nt sequence (nt 262–550) of the promoter contains the cis-acting elements essential for BNip3 gene expression.

We next determined the cis-acting elements responsive to MHV infection. Cells were transfected with the full-length and various deletion reporter constructs for 5 h and were then infected with UV-inactivated MHV at an m.o.i. of 5 or mock-infected as controls. As shown in Fig. 6, the luciferase activities were decreased approximately four- to sixfold in MHV-infected cells for various reporter constructs (full-length, Pr-7, Pr-4, Pr-10, Pr-15, and Pr-6), as compared with those in mock-infected control cells. The reduction of luciferase activities must have resulted from the infection process rather than from general inhibition by MHV replication, because the virus was inactivated by UV

irradiation. These results suggest that the negative elements responsive to MHV infection reside within the same region of the promoter that is required for BNip3 expression. We were unable to narrow down further the minimal responsive elements because further deletions within this region in the reporter constructs drastically abrogate the reporter gene expression even in the absence of virus infection (constructs Pr-5, Pr-11, Pr-12, Pr-14, Pr-13, and Pr-9).

Discussion

In this study, we employed DNA microarray, RT–PCR, Western blot, and a promoter–reporter gene system to explore the potential alteration of cellular gene expression by MHV infection. Using such multitude approaches, we discovered that the expression of the cellular proapoptotic gene BNip3 was significantly down-regulated in cultured DBT cells by MHV infection. This finding supports the hypothesis that MHV infection in DBT cells may induce an anti-

apoptotic state through down-regulation of expression of proapoptotic genes. It has been shown that MHV infection induces apoptosis in macrophages and fibroblast cells but not in DBT cells (Belyavsky, et al., 1998; An et al., 1999; Chen and Makino, 2002). However, overexpression of the single viral E protein in DBT cells by a recombinant vaccinia virus results in apoptosis, which can be blocked by overexpression of an antiapoptotic protein Bcl-2, indicating the involvement of the mitochondrial pathway in E protein-induced apoptosis in DBT cells (An et al., 1999). How MHV infection in DBT cells overcomes the apoptotic effect induced by the E protein expression remained unanswered in that study. It is possible that MHV infection of DBT cells induces an antiapoptotic state during an early stage of the virus life cycle through down-regulation of proapoptotic genes such as BNip3 (this study) or up-regulation of anti-apoptotic genes (Cai and Zhang, unpublished results). Such an antiapoptotic response would prevent cells from succumbing to apoptosis induced by the viral apoptotic E protein. Consistent with this hypothesis is the observation that when DBT cells were treated with apoptotic inducers, fewer cells underwent apoptosis when infected with MHV than mock-infected cells (Cai and Zhang, unpublished results). Although a direct correlation between down-regulation of BNip3 and inhibition of E protein-induced apoptosis in DBT cells has not been determined, the general proapoptotic effect exerted by BNip3 (Chen et al., 1997; Mizutani et al., 2002; Kubasiak et al., 2002; Lamy et al., 2003) makes the hypothesis conceivable. Moreover, the involvement of the mitochondrial/Bcl-2 pathway in E protein-induced apoptosis correlates well with the functional role of BNip3 as a member of the proapoptotic, mitochondrial/Bcl-2 family. Thus, it is conceivable that down-regulation of BNip3 expression can shift the balance to an antiapoptotic state at the mitochondrial checkpoint.

Using UV-inactivated virus for infection and chloroquine for blocking the acidification of the endosomes, we demonstrated that the down-regulation of BNip3 gene expression by OBLV60 infection was mediated during cell entry and required no virus replication (Figs. 4 and 5). However, treatment of DBT cells with chloroquine did not completely block the down-regulation of BNip3 expression by OBLV60 infection (Fig. 5). One possible interpretation is that a part of the signals that trigger the down-regulation of BNip3 expression has already been induced during virus attachment and endocytosis but prior to fusion between viral envelope and endosomal membranes (in the case of OBLV60 virus), so that inhibition of fusion by chloroquine cannot completely derepress the BNip3 promoter activity. Alternatively, the partial restoration of BNip3 promoter activity may be due to incomplete blockage of fusion by chloroquine. This is possible and even likely because the virus infectivity was reduced by approximately only 1 log10 by chloroquine treatment (at 50 μM). Although Gallagher et al. (1991) reported a reduction of 3 log10 in virus titer when DBT cells were treated with chloroquine at 50 μM, they

used approximately 3 log10 less virus for infection. In our infection–transfection experiments, we had to use a higher m.o.i. to insure that each transfected cell is infected with a virus. The higher virus infectivity used in this study likely contributes to a lesser effective inhibition by chloroquine. Therefore, although it cannot exclude the possibility that virus attachment to cell receptors and the subsequent endocytosis are also involved in signaling BNip3 down-regulation, our results clearly establish that virus–cell fusion during entry triggers the signaling cascade.

Little is known about the cis-acting elements that regulate BNip3 gene expression. Our systematic deletion analyses identified the 288-nt sequence (from nt 262 to 550) of the BNip3 promoter, which is necessary and sufficient for the expression of BNip3 gene. Interestingly, this region also contains the two previously identified hypoxia response elements (HRE-1 and HRE-2) (Bruick, 2000), the TATA box, four transcription factor Sp1-binding sites, the CAC or CCACC consensus sequence, the CCAAT box, and the nuclear factor- (NF) 1-binding site (Fig. 6B). It is not known whether and how these transcription factors are involved in the regulation of BNip3 gene expression. It has been reported that the transcription factor hypoxia-inducing factor-1 binds to the HREs on the BNip3 promoter and induces the BNip3 expression (Bruick, 2000; Kubasiak et al., 2002), whereas the zinc-finger protein PLAGL2 induces the expression of BNip3 via the same HREs, but independent of the hypoxia-inducing factor-1 (Mizutani et al., 2002). Our finding that further deletions within this 288-nt region inactivated the promoter suggests that BNip3 transcription in DBT cells likely requires multiple transcription factors acting in concert with these cis-elements.

The mechanism by which MHV infection of DBT cells downregulates BNip3 gene expression is currently unknown. We have attempted to identify the negative elements that are responsive to MHV infection. Our results showed that the negative, MHV-responsive elements largely overlap with the cis-acting elements essential for BNip3 transcription (Fig. 6). One hypothesis is that MHV infection triggers the induction of one or more transcription factors that act on the 288-nt sequence of the BNip3 promoter to compete with the positive transcription regulators, thereby down-regulating the transcription of BNip3 on infection. In our DNA microarray analysis, we found that the expression of a class of early response transcription factors such as *c-fos* (12-fold increase) and early growth response gene-1 (*Egr-1*) (9-fold increase) was significantly induced by MHV infection (data not shown). Preliminary studies employing transient cotransfection of DBT cells with plasmids expressing *c-fos* or *Egr-1* gene and the BNip3 promoter reporter plasmid demonstrated that the BNip3 promoter was down-regulated by Egr-1 in a dose-dependent manner but not by c-fos, suggesting that the down-regulation of BNip3 gene expression by MHV infection might be mediated through the induction of Egr-1 (data not shown). It has been shown that Egr-1 and Sp1 share the consensus

binding sequence and that Egr-1 can act as an antagonist of Sp1 by binding to the Sp1 consensus sequence and represses transcription (Huang et al., 1997). Our analysis of the 288-nt BNip3 promoter sequence (from nt 262 to nt 550) identified four Sp1-binding sites: two upstream at nt 285 and 320 and two downstream at nt 441 and 496, respectively. Coincidently, MHV infection of DBT cells inhibited the luciferase expression in all reporter plasmids that contain the two or four Sp1-binding sites (Fig. 6). However, direct evidence for the role of Egr-1 in MHV-dependent transcriptional regulation of BNip3 gene remains to be established. A recent study showed that overexpression of Egr-1 resulted in down-regulation of BNip3 transcription in prostate cancer cells (Virolle et al., 2003), thus providing supporting evidence for the role of Egr-1 in regulating BNip3 gene.

Materials and methods

Viruses, cells, and antibodies

The mouse hepatitis virus (MHV) strain JHM (Makino and Lai, 1989) was used throughout this study. For some experiments, MHV strain A59 (Leibowitz et al., 1981) and the mutant OBLV60 (Gallagher et al., 1991) were also used. OBLV60 (kindly provided by Michael Buchmeier, The Scripps Research Institute, La Jolla, California) was originally isolated from the OBL20 cells that were persistently infected with MHV JHM (MHV-4). This mutant enters cells via receptor-mediated endocytosis and thus its entry depends on acidic pH. The mouse astrocytoma cell line (DBT) (Hirano et al., 1974) was used for virus propagation, plaque assay, and all other experiments involving cell culture throughout this study. DBT cells were cultured in 1X minimum essential medium (MEM) containing 10% trypton phosphate broth (TPB) and 7.5% newborn calf serum (NCS) (Gibco BRL, Gaithersburg, MD). All MHV strains were propagated in DBT cells in MEM either containing 1% NCS or serum-free. For propagation of OBLV60 mutant virus, no $NaHCO_3$ was added to the medium. A recombinant vesicular stomatitis virus (VSV) expressing the green fluorescence protein (GFP) originally provided by Michael Whitt (University of Tennessee at Memphis) was obtained from Marie Chow (UAMS). VSV was propagated and titered in Hela cells. Antibodies specific to mouse BNip3 protein and β-actin were purchased from Santa Cruz Biochem and Sigma, respectively.

RNA isolation and purification

DBT cells were infected with MHV at a multiplicity of infection (m.o.i.) of 5 or mock-infected. At various time points postinfection (p.i.), intracellular total RNAs were isolated and purified with the RNeasy kit according to the manufacturer's instruction (Qiagen, Inc.). RNAs were then treated with RNase-free DNase I (Promega). The concen-

trations of the RNA samples were determined by spectrophotometry (Hitatchi, Model No. 4500).

Reverse transcription and polymerase chain reaction (RT–PCR)

For detection of the proapoptotic gene BNip3 mRNA, a semiquantitative, competitive RT–PCR was employed. Briefly, the RNAs were reverse-transcribed into cDNAs with Maloney murine leukemia virus (MMLV) reverse transcriptase (Promega) by using a random hexomer oligonucleotide primer (Invitrogen, Inc.) in a standard RT reaction as described previously (Zhang et al., 1991). cDNAs were then used as templates for PCR amplification with two pairs of primers specific for BNip3 gene and β-actin gene as an internal control, respectively. The sense primer for BNip3 (5′BNip3-RT: 5′-CAG GGC TCC TGG GTA GAA CT-3′) corresponds to a sequence at nucleotides (nt) 28–47 of the open reading frame (ORF), and the antisense primer (3′BNip3-RT: 3′-GCA GAT GAG ACA GTA ACA GAG-3′) is complementary to a sequence at nt 482–502 according to the published sequence (GenBank accession number: AF041054). Thus, the PCR product is 474 nt in length. The primer pair for β-actin is 5′mb-actin (5′-ACC AAC TGG GAC GAT ATG GAG AAG A-3′, corresponding to the sequence at nt 229–253) and 3′mb-actin (5′-TAC GAC CAG AGG CAT ACA GGG ACA-3′, complementary to a sequence at nt 418–442 of the β-actin gene) (GenBank accession number: NM007393). The PCR product for the β-actin gene is 215 nt in length. PCR was carried out in a reaction of 20 μl containing 1X PCR buffer (20 mM Tris–HCl, pH 8.3, 25 mM KCl, 1.5 mM $MgCl_2$, 0.1% Tween-20), 200 μM each of the four dNTPs, 20 pM of primers, 3U of *Taq* DNA polymerase, 2 μl of the RT products, for 30 cycles with each cycle consisting of denaturation at 95°C for 20 s, annealing at 55°C for 1 min and extension at 72°C for 1 min with a final extension of 10 min. PCR was performed in a thermocycler DNA engine (Model PTC-200, MJ Research). For competitive PCR, a plasmid DNA containing a 99-nt deletion between the primer sequences (5′BNip3 and 3′BNip3) was constructed (see below) and used as a competitor. For each RNA sample, at least 10 PCR reactions were performed with an incremental amount of the competitor DNA. PCR products were analyzed by agarose gel electrophoresis, and the gels were stained with ethidium bromide and photographed with a UVP gel document center. The intensity of the DNA bands was determined by densitometry, analyzed with manufacture-installed software (UVP), and plotted. The point at which the amount of target PCR products equals to a known amount of competitor DNA being added in the PCR reaction is the amount of target cDNA of the virus-infected cells, which is expressed as percentage relative to the amounts of target cDNA in mock-infected cells (which were set as 100%).

UV inactivation of MHV

MHV strains JHM and A59 and VSV were inactivated by exposing the viruses to UV light for 30 min on ice in a UV crosslinker (Fisher Scientific). Inactivation was confirmed by titration of samples before and after UV-light exposure and by the absence of cytopathic effect after inoculation of DBT cell monolayers with UV-irradiated virus or by the absence of green fluorescence cells (for VSV).

Immunoprecipitation and Western blot analysis

DBT cells were grown to monolayer in 60-mm Petri dishes and were infected with MHV JHM at an m.o.i. of 5 or mock-infected. At 5, 9, and 13 h p.i., cells were harvested and lysed in 500 μl of radioimmunoprecipitation assay (RIPA) buffer (50 mM Tris–HCl, pH 7.5, 150 mM NaCl, 0.5% sodium deoxycholate, 1% NP-40) containing protease inhibitor cocktail tablets (Roche, Mannheim, Germany). The cell lysates were passed through a 25-gauge needle several times to sheer the DNA and were clarified from cell debris by centrifugation. The protein concentration was measured by using Bio-Rad protein assay kit (Bio-Rad, CA). Equal amounts of cell lysates (cell number equivalent) were immunoprecipitated with an anti-BNip3 peptide antibody (2 μg/ml) (Santa Cruz, CA) for 1 h at 4°C in a rocking platform (Bellco Inc.). The antigen–antibody complexes were then precipitated with protein G-Sepharose beads (10 μl of the 50% slurry) (Roche) for 4 h at 4°C in a rocking platform. Protein G beads were pelleted down by centrifugation and washed three times with the RIPA buffer. Twenty microliter of 1X protein sample loading buffer [10 mM Tris–HCl, pH 6.8, 100 mM dithiothreitol (DTT), 2% sodium dodecyl sulfate (SDS), 0.1% bromphenol blue, 10% glycerol] were added to each sample. Samples were boiled for 3 min, chilled on ice, and pelleted by centrifugation before loading onto gels. Proteins were separated by SDS–polyacrylamide gel (12%) electrophoresis (PAGE). The proteins were then transferred to nitrocellulose membrane (MSI, Westborough, MA) for 4 h at 100 V in a transfer buffer (25 mM Tris, 200 mM glycine, 20% methanol, 0.02% SDS). After being blocked with 5% skin milk in Tris-buffered saline (TBS) for 1 h at room temperature, the membrane was washed three times in TBS containing 0.5% Tween-20 and immunoblotted with the BNip3 antibody (1 μg/ml) for 2 h at room temperature, followed by a secondary Ab coupled to horseradish peroxidase (1:1000 dilution) (Sigma) for 1 h at room temperature. The presence of the BNip3 protein was detected by enhanced chemiluminescence (ECL) using peracid as a substrate (Amersham) followed by autoradiography.

Plasmid construction

The luciferase reporter plasmid that contains 588 nt 5′ upstream sequence (the promoter) of BNip3 gene in front of the luciferase ORF was kindly provided by Richard Bruick (University of Texas, Southwestern Medical Center in Dallas). For construction of a competitor DNA for quantitative PCR, the full-length ORF of BNip3 gene was cloned. RNAs were isolated from DBT cells and cDNAs were synthesized by RT using the random hexomer primer described above. The BNip3 gene was amplified by PCR using the sense primer 5′BNip3*Eco*RI (5′-AGT <u>GAA TTC</u> ACC ATG TCG CAG AGC-3′, corresponding to the first 15 nt of the BNip3 ORF, GenBank accession number AF041054), which contains an *Eco*RI site at the 5′-end (underlined), and the antisense primer 3′BNip3*Xho*I (5′-<u>CTC GAG</u> GAA GGT GCT AGT GGA-3, complementary to the last 15 nt of the BNip3 ORF), which contains an *Xho*I site (underlined). The PCR products were directly cloned into pCR2.1 TA cloning vector (Invitrogen), resulting in pTA-BNip3. The sequence of the clone was confirmed by automatic DNA sequencing (IBI, Prizm-377) in the Departmental Core Facility. An internal deletion was made in three steps. In the first PCR, a 222-nt fragment of the BNip3 gene was amplified from the full-length clone pTA-BNip3 using the primer pair 5′BNip3-RT and 3′BNip3-Cl (5′-TTT CTC GCC AAA GCT GTG GC-3′, complementary to the sequence at nt 230–249). In the second PCR, a 173-nt fragment of the BNip3 gene was synthesized using the primer pair 5′BNip3-Cl (5′-GC CAC AGC TTT GGC GAG AAA CCA GAA AAT ATT CCC CCC AAG-3′, corresponding to sequence at nt 349–369 with a 20-nt sequence overhang at the 5′-end that corresponds to nt 230–249) and 3′BNip3-RT. The PCR products from these two sets of reactions were separated by agarose gel electrophoresis; the corresponding DNA fragments were excised from the gels and purified with a gel extraction kit (Qiagen, Inc.). The two PCR fragments were then mixed and used as templates for a third PCR. The third PCR was carried out with the primer pair 5′BNip3-RT and 3′BNip3-RT. The products from the third PCR were directly cloned into the pCR2.1-TA cloning vector (Invitrogen), resulting in generation of pTA-BNip3D100. This clone contains the region of BNip3 gene from nt 28 to nt 502 with a deletion between nt 249 and nt 349. This clone was then used as a competitor for the competitive PCR described above.

For construction of 5′-deletion mutants of the BNip3 promoter, plasmid pGL3-BNip3, which contains the full-length promoter, was doubly digested with *Hin*dIII and *Bst*XI, *Pf1*MI, or *Stu*I, respectively. The digested plasmids were purified with the gel extraction kit (Qiagen) following agarose gel electrophoresis, blunt-ended with T4 DNA polymerase, and self religated with T4 DNA ligase, resulting in generation of pGL3-BNip3-Pr7, pGL3-BNip3-Pr4, and pGL3-BNip3-Pr5, respectively (Fig. 6). Deletion mutants pGL3-BNip3-Pr10, pGL3-BNip3-Pr11, pGL3-BNip3-Pr12, pGL3-BNip3-Pr14, pGL3-BNip3-Pr15, and pGL3-BNip3-Pr6 were made similarly by deleting the internal fragments through double digestion with *Stu*I and *Nco*I, Pf1 MI and *Nco*I, *Bst*XI and *Nco*I, *Pf1*MI and *Stu*I, *Bst*XI and

Pfl MI, or *Apa*I alone (two sites), respectively. For construction of pGL3-BNip3-Pr13 and pGL3-BNip3-Pr9, the 138-nt *Pfl*MI–*Stu*I fragment and the 224-nt *Apa*I–*Apa*I fragment were blunt-ended and cloned into the *Sma*I site of the pGL3-Basic vector. The orientation of these fragments in the plasmids were confirmed by DNA sequencing.

DNA transfection and luciferase assay

For DNA transfection, the LipofectAmine reagent was used according to the manufacturer's instruction (Gibco-Life Technologies, Inc.). Briefly, DBT cells were seeded in a 24-well culture plates at a density of 4×10^5 cells per well. When the cells reached to approximately 60% confluency, ≈500 ng of plasmid DNAs and 3 μl of the LipofectAmine reagent were diluted separately in 100 μl of serum-free OPTI medium without antibiotics, mixed, and incubated at room temperature for 30 min before adding to each well of the 24-well plate. DBT cells were washed with PBS and 300 μl of OPTI medium were added to each well of the cell culture. The DNA–lipofect Amine mixture (200 μl) was added to each well and the cell culture plates were incubated at 37°C for various time periods as indicated. For luciferase assay, cells were harvested along with culture medium and lysed by freezing and thawing. One hundred microliters of the cell lysate was assayed for luciferase activity using the Luciferase Assay System (Promega) in a microtiter plate Luminometer (Dynex Technologies, Inc.).

Acknowledgments

References

Adami, C., Pooley, J., Glomb, J., Stecker, E., Fazal, F., Fleming, J.O., Baker, S., 1995. Evolution of mouse hepatitis virus (MHV) during chronic infection: quasispecies nature of the persisting MHV RNA. Virology 209, 337–346.

An, S., Chen, C.J., Yu, X., Leibowitz, J.L., Makino, S., 1999. Induction of apoptosis in murine coronavirus-infected cultured cells and demonstration of E protein as an apoptosis inducer. J. Virol. 73, 7853–7859.

Belyavsky, M., Belyavskaya, E., Levy, G.A., Leibowitz, J.L., 1998. Coronavirus MHV-3-induced apoptosis in macrophages. Virology 250, 41–49.

Bos, E.C., Luytjes, W., Van der Meulen, H.V., Koerten, H.K., Spaan, W.J., 1996. The production of recombinant infectious DI-particles of a murine coronavirus in the absence of helper virus. Virology 218, 52–60.

Boyd, J.M., Malstrom, S., Subramanian, T., Venkatesh, L.K., Schaeper, U., Elangovan, B., D'Sa-Eipper, C., Chinnadurai, G., 1994. Adenovirus E1B 19 kDa and Bcl-2 proteins interact with a common set of cellular proteins. Cell 79, 341–351.

Bruick, R.K., 2000. Expression of the gene encoding the proapoptotic Nip3 protein is induced by hypoxia. Proc. Natl. Acad. Sci. USA 97, 9082–9087.

Chen, C.J., Makino, S., 2002. Murine coronavirus-induced apoptosis in 17Cl-1 cells involves a mitochondria-mediated pathway and its downstream caspase-8 activation and bid cleavage. Virology 302, 321–332.

Chen, G., Ray, R., Dubik, D., Shi, L., Cizeau, J., Bleackley, R.C., Saxena, S., Gietz, R.D., Greenberg, A.H., 1997. The E1B 19K/Bcl-2-binding protein Nip3 is a dimeric mitochondrial protein that activates apoptosis. J. Exp. Med. 186, 1975–1983.

Chen, G., Ray, R., Dubik, D., Shi, L., Cizeau, J., Bleackley, R.C., Saxena, S., Gietz, R.D., Greenberg, A.H., 1997. The E1B 19K/Bcl-2-binding protein Nip3 is a dimeric mitochondrial protein that activates apoptosis. J. Exp. Med. 186, 1975–1983.

Chen, Y., Swanson, R.A., 2003. Astrocytes and Brain Injury. J. Cerebr. Blood Flow Metab. 23, 137–149.

Chen, W., Baric, R.S., 1996. Molecular anatomy of mouse hepatitis virus persistence: coevolution of increased host cell resistance and virus virulence. J. Virol. 70, 3947–3960.

Chen, W., Baric, R.S., 1995. Function of a 5'-end genomic RNA mutation that evolves during persistent mouse hepatitis virus infection in vitro. J. Virol. 69, 7529–7540.

Chiou, S.K., Tseng, C.C., Rao, L., White, E., 1994. Functional complementation of the adenovirus E1B 19-kilodalton protein with Bcl-2 in the inhibition of apoptosis in infected cells. J. Virol. 68, 6553–6566.

Fierz, W., Endler, B., Reske, K., Wekerle, H., Fontana, A., 1985. Astrocytes as antigen-presenting cells. I. Induction of Ia antigen expression on astrocytes by T cells via immune interferon and its effect on antigen presentation. J. Immunol. 134, 3785–3793.

Fleming, J.O., Houtman, J.J., Alaca, H., Hinze, H.C., McKenzie, D., Aiken, J., Bleasdale, T., Baker, S., 1993. Persistence of viral RNA in the central nervous system of mice inoculated with MHV-4. Adv. Exp. Med. Biol. 342, 327–332.

Gallagher, T.M., Escarmis, C., Buchmeier, M.J., 1991. Alteration of the pH dependence of coronavirus-induced cell fusion: effect of mutations in the spike glycoprotein. J. Virol. 65, 1916–1928.

Grzybicki, D.M., Kwack, K.B., Perlman, S., Murphy, S.P., 1997. Nitric oxide synthase type II expression by different cell types in MHV-JHM encephalitis suggests distinct roles for nitric oxide in acute versus persistent virus infection. J. Neuroimmunol. 73, 15–27.

Henderson, S., Rowe, M., Gregory, C., Croom-Carter, D., Wang, F., Longnecker, R., Kieff, E., Rickinson, A., 1991. Induction of bcl-2 expression by Epstein–Barr virus latent membrane protein 1 protects infected B cells from programmed cell death. Cell 65, 1107–1115.

Herndon, R.M., Price, D.L., Weiner, L.P., 1977. Regeneration of oligodendroglia during recovery from demyelinating disease. Science 195, 693–694.

Hilton, A., Mizzen, L., MacIntyre, G., Cheley, S., Anderson, R., 1986. Translational control in murine hepatitis virus infection. J. Gen. Virol. 67, 923–932.

Hirano, N., Fujiwara, K., Hino, S., Matumoto, M., 1974. Replication and plaque formation of mouse hepatitis virus (MHV-2) in mouse cell line DBT culture. Arch. Gesamte Virusforsch. 44, 298–302.

Hockenbery, D., Nunez, G., Milliman, C., Schreiber, R.D., Korsmeyer, S.J., 1990. Bcl-2 is an inner mitochondrial membrane protein that blocks programmed cell death. Nature 348, 334–336.

Huang, D., Han, Y., Rani, M.R., Glabinski, A., Trebst, C., Sorensen, T., Tani, M., Wang, J., Chien, P., O'Bryan, S., Bielecki, B., Zhou, Z.L., Majumder, S., Ransohoff, R.M., 2000. Chemokines and chemokine receptors in inflammation of the nervous system: manifold roles and exquisite regulation. Immunol. Rev. 177, 52–67.

Huang, R.P., Fan, Y., Ni, Z., Mercola, D., Adamson, E.D., 1997. Reciprocal modulation between Sp1 and Egr-1. J. Cell Biochem. 66, 489–499.

Imazu, T., Shimizu, S., Tagami, S., Matsushima, M., Nakamura, Y., Miki, T., Okuyama, A., Tsujimoto, Y., 1999. Bcl-2/E1B 19 kDa-interacting protein 3-like protein (Bnip3L) interacts with bcl-2/Bcl-xL and induces apoptosis by altering mitochondrial membrane permeability. Oncogene 18, 4523–4529.

Joseph, J., Grun, J.L., Lublin, F.D., Knobler, R.L., 1993. Interleukin-6 induction in vitro in mouse brain endothelial cells and astrocytes by exposure to mouse hepatitis virus (MHV-4, JHM). J. Neuroimmunol. 42, 47–52.

Kalicharran, K., Dales, S., 1995. Dephosphorylation of the nucleocapsid protein of inoculum JHMV may be essential for initiating replication. Adv. Exp. Med. Biol. 380, 485–489.

Kalicharran, K., Mohandas, D., Wilson, G., Dales, S., 1996. Regulation of the initiation of coronavirus JHM infection in primary oligodendrocytes and L-2 fibroblasts. Virology 225, 33–43.

Kelekar, A., Thompson, C.B., 1998. Bcl-2-family proteins: the role of the BH3 domain in apoptosis. Trends Cell Biol. 8, 324–330.

Kubasiak, L.A., Hernandez, O.M., Bishopric, N.H., Webster, K.A., 2002. Hypoxia and acidosis activate cardiac myocyte death through the Bcl-2 family protein BNip3. Proc. Natl. Acad. Sci. USA 99, 12825–12830.

Kyuwa, S., Cohen, M., Nelson, G., Tahara, S.M., Stohlman, S.A., 1994. Modulation of cellular macromolecular synthesis by coronavirus: implication for pathogenesis. J. Virol. 68, 6815–6819.

La Monica, N., Yokomori, K., Lai, M.M.C., 1992. Coronavirus mRNA synthesis: identification of novel transcription initiation signals which are differentially regulated by different leader sequences. Virology 188, 402–407.

Lai, M.M.C., 1990. Coronaviruses: Organization, replication and expression of genome. Annu. Rev. Microbiol. 44, 303–333.

Lampert, P.W., Sims, J.K., Kniazeff, A.J., 1973. Mechanism of demyelination in JHM virus encephalomyelitis: electron microscopic studies. Acta Neuropathol. (Berl.) 24, 76–85.

Lamy, L., Ticchioni, M., Rouquette-Jazdanian, A.K., Samson, M., Deckert, M., Greenberg, A., Bernard, A., 2003. CD47 and the BH3-only protein BNIP3 in T-cell apoptosis. J. Biol. Chem. Published online on April 10, 2003.

Leibowitz, J.L., Wilhelmsen, K.C., Bond, C.W., 1981. The virus-specific intracellular RNA species of two murine coronaviruses: MHV-a59 and MHV-JHM. Virology 114, 39–51.

Luytjes, W., Bredenbeek, P.J., Noten, A.F., Horzinek, M.C., Spaan, W.J., 1988. Sequence of mouse hepatitis virus A59 mRNA 2: indications for RNA recombination between coronaviruses and influenza C virus. Virology 166, 415–422.

Maeda, A., Hayashi, M., Ishida, K., Mizutani, T., Watanabe, T., Namioka, S., 1995. Characterization of DBT cell clones derived from cells persistently infected with the JHM strain of mouse hepatitis virus. J. Vet. Med. Sci. 57, 813–817.

Makino, S., Lai, M.M.C., 1989. Evolution of the 5′-end of genomic RNA of murine coronaviruses during passages in vitro. Virology 169, 227–232.

Mizutani, A., Furukawa, T., Adachi, Y., Ikehara, S., Taketani, S., 2002. A zinc-finger protein, PLAGL2, induces the expression of a proapoptotic protein Nip3, leading to cellular apoptosis. J. Biol. Chem. 277, 15851–15858.

Nash, T.C., Buchmeier, M.J., 1997. Entry of mouse hepatitis virus into cells by endosomal and nonendosomal pathways. Virology 233, 1–8.

Niemann, H., Geyer, R., Klenk, H.D., Linder, D., Stirm, S., Wirth, M., 1984. The carbohydrates of mouse hepatitis virus (MHV) A59: structures of the O-glycosidically linked oligosaccharides of glycoprotein E1. EMBO J. 3, 665–670.

Perlman, S., Ries, D., 1987. The astrocyte is a target cell in mice persistently infected with mouse hepatitis virus, strain JHM. Microb. Pathogen. 3, 309–314.

Prestridge, D.S., 2000. Computer software for eukaryotic promoter analysis. Method Mol. Biol. 130, 265–295.

Riedel, H., Kondor-Koch, C., Garoff, H., 1984. Cell surface expression of fusogenic vesicular stomatitis virus G protein from cloned cDNA. EMBO J. 3, 1477–1483.

Rowe, C.L., Baker, S.C., Nathan, M.J., Sgro, J.Y., Palmenberg, A.C., Fleming, J.O., 1998. Quasispecies development by high frequency RNA recombination during MHV persistence. Adv. Exp. Med. Biol. 440, 759–765.

Sawicki, S.G., Lu, J.H., Holmes, K.V., 1995. Persistent infection of cultured cells with mouse hepatitis virus (MHV) results from the epigenetic expression of the MHV receptor. J. Virol. 69, 5535–5543.

Shieh, C.K., Lee, H.J., Yokomori, K., La Monica, N., Makino, S., Lai, M.M.C., 1989. Identification of a new transcriptional initiation site and the corresponding functional gene 2b in the murine coronavirus RNA genome. J. Virol. 63, 3729–3736.

Shimizu, S., Narita, M., Tsujimoto, Y., 1999. Bcl-2 family proteins regulate the release of apoptogenic cytochrome c by the mitochondrial channel VDAC. Nature 399, 483–487.

Silins, S.L., Sculley, T.B., 1995. Burkitt's lymphoma cells are resistant to programmed cell death in the presence of the Epstein–Barr virus latent antigen EBNA-4. Int. J. Cancer 60, 65–72.

Stohlman, S.A., Lai, M.M.C., 1979. Phosphoproteins of murine hepatitis viruses. J. Virol. 32, 672–675.

Tahara, S.M., Dietlin, T.A., Bergmann, C.C., Nelson, G.W., Kyuwa, S., Anthony, R.P., Stohlman, S.A., 1994. Coronavirus translational regulation: leader affects mRNA efficiency. Virology 202, 621–630.

Van Wagoner, N.J., Benveniste, E.N., 1999. Interleukin-6 expression and regulation in astrocytes. J. Neuroimmunol. 100, 124–139.

Virolle, T., Krones-Herzig, A., Baron, V., De Gregorio, G., Adamson, E.D., Mercola, D., 2003. Egr1 promotes growth and survival of prostate cancer cells. Identification of novel Egr1 target genes. J. Biol. Chem. 278, 11802–11810.

Vennema, H., Godeke, G.J., Rossen, J.W., Voorhout, W.F., Horzinek, M.C., Opstelten, D.J., Rottier, P.J., 1996. Nucleocapsid-independent assembly of coronavirus-like particles by co-expression of viral envelope protein genes. EMBO J. 15, 2020–2028.

Williams, R.K., Jiang, G.S., Holmes, K.V., 1991. Receptor for mouse hepatitis virus is a member of the carcinoembryonic antigen family of glycoproteins. Proc. Natl. Acad. Sci. USA 88, 5533–5536.

Woyciechowska, J.L., Trapp, B.D., Patrick, D.H., Shekarchi, I.C., Leinikki, P.O., Sever, J.L., Holmes, K.V., 1984. Acute and subacute demyelination induced by mouse hepatitis virus strain A59 in C3H mice. J. Exp. Pathol. 1, 295–306.

Yasuda, M., Theodorakis, P., Subramanian, T., Chinnadurai, G., 1998. Adenovirus E1B-19K/BCL-2 interacting protein BNIP3 contains a BH3 domain and a mitochondrial targeting sequence. J. Biol. Chem. 273, 12415–12421.

Yokomori, K., La Monica, N., Makino, S., Shieh, C.K., Lai, M.M.C., 1989. Biosynthesis, structure, and biological activities of envelope protein gp65 of murine coronavirus. Virology 173, 683–691.

Yokomori, K., Banner, L.R., Lai, M.M.C., 1991. Heterogeneity of gene expression of the hemagglutinin-esterase (HE) protein of murine coronaviruses. Virology 183, 647–657.

Yu, X., Bi, W., Weiss, S.R., Leibowitz, J.L., 1994. Mouse hepatitis virus gene 5b protein is a new virion envelope protein. Virology 202, 1018–1023.

Zauli, G., Gibellini, D., Caputo, A., Bassini, A., Negrini, M., Monne, M., Mazzoni, M., Capitani, S., 1995. The human immunodeficiency virus type-1 Tat protein upregulates Bcl-2 gene expression in Jurkat T-cell lines and primary peripheral blood mononuclear cells. Blood 86, 3823–3834.

Zhang, X.M., Kousoulas, K.G., Storz, J., 1991. Comparison of the nucleotide and deduced amino acid sequences of the S genes specified by virulent and avirulent strains of bovine coronaviruses. Virology 183, 397–404.

Zhou, J., Stohlman, S.A., Marten, N.W., Hinton, D.R., 2001. Regulation of matrix metalloproteinase (MMP) and tissue inhibitor of matrix metalloproteinase (TIMP) genes during JHMV infection of the central nervous system. Adv. Exp. Med. Biol. 494, 329–334.